



Cite this: *New J. Chem.*, 2021, **45**, 4347

# A fluorogenic probe for dynamic tracking of lipid droplets' polarity during the evolution of cancer†

Cong Liu, <sup>a</sup> Junling Yin, <sup>a</sup> Bingli Lu <sup>a</sup> and Weiyong Lin <sup>\*ab</sup>

Exploring the changes in the polarity of intracellular lipid droplets (LDs) during the evolution of cancer is important for cancer detection and treatment. Therefore, we designed and synthesized a new type of polarity-sensitive fluorescent probe, **CTPE**, which uses coumarin as the polarity-sensitive group and tetraphenylethylene as the electron-donating group to target LDs. Due to its special intramolecular charge transfer mechanism, **CTPE** emitted a weak green fluorescence in high-polar solvents, and a strong green fluorescence in low-polar solvents, thus exhibiting a drastic change in fluorescence signal as a function of the solvent polarity. In virtue of the probe **CTPE**, tumorous tissues have been successfully identified from normal ones and the decrease in LDs' polarity could be revealed with the evolution of cancer. Moreover, the changes in the LDs' polarity in drugs-treated tumor were observed at the tissue level, endowing its capacity for anti-cancer drug efficacy evaluation. This work provides a promising imaging tool for LDs tracking in cancer research and clinical diagnosis.

Received 3rd December 2020,  
 Accepted 26th January 2021

DOI: 10.1039/d0nj05900e

rsc.li/njc

## 1. Introduction

Cancer is recognized as a severe disease with high mortality rate, which is often a consequence of late diagnosis during advanced stages.<sup>1,2</sup> The timely diagnosis of cancer is critical such that effective treatment therapy can be initiated in early stages without locally advancing the disease or metastasis. Therefore, it is necessary to detect cancer in time to improve the survival rate.<sup>3</sup> Accordingly, performing relevant research to explore cancer evolution is highly desirable for current medical diagnostics. In recent years, cancer detection through related markers has become a hot topic, which has been studied in more and less economically developed countries alike. At present, a large number of tumor markers have been discovered through genomic and proteomic studies, which greatly facilitates the diagnosis of cancer.<sup>4–6</sup> However, most of them fail to effectively detect cancer because of their invasive, unpleasant, and inconvenient nature.<sup>7</sup> Therefore, it is particularly important to develop a new strategy to identify tumors.

Lipid droplets (LDs) are cellular organelles that store lipids comprising a core of neutral lipids surrounded by a monolayer of phospholipids loaded with associated proteins.<sup>8,9</sup> In addition to energy storage, LDs participate in physiological processes such as cell activation, migration, proliferation, and apoptosis.<sup>10,11</sup> Abnormal LDs can be detected in diseases such as type II diabetes, obesity, and atherosclerosis. Especially, due to specific alterations in the metabolic activity in cancer cells, parameters related to LDs should be quite different from those of normal cells.<sup>12–17</sup> Recent evidence suggests that lipid biosynthesis gets dysregulated because of the development of cancer and reactivation of lipid biosynthesis is frequently observed in cancer tissue. The excess of LDs in a cancer cell is attributed to the enhanced rate of glycolysis producing pyruvate, known as the Warburg effect.<sup>18,19</sup> It should also be noted that the abnormal lipid content leads to the variation in hydrophilic and hydrophobic domains in the LD, further leading to the change in the polarity of LDs. Although increasing contribution has been devoted to the study of the metabolic processes involved in LDs and their regulation within the context of cancer, the potential role of LDs' polarity in tumor progression have not yet been fully understood.<sup>20–23</sup> Thus, timely attention should be given to the study of the LDs' polarity during the evolution of cancer.

Fluorescence imaging technology is a highly sensitive characterization technique with the ability to perform non-destructive, real-time and *in situ* detection of target analytes, and has become a powerful tool for understanding biological systems with high spatial resolution.<sup>24–27</sup> Therefore, it can serve as a feasible strategy to develop a new tool for studying the

<sup>a</sup> Institute of Fluorescent Probes for Biological Imaging, School of Chemistry and Chemical Engineering, School of Materials Science and Engineering, University of Jinan, Jinan, Shandong, 250022, People's Republic of China. E-mail: weiyonglin2013@163.com

<sup>b</sup> Guangxi Key Laboratory of Electrochemical Energy Materials, Institute of Optical Materials and Chemical Biology, School of Chemistry and Chemical Engineering, Guangxi University, Nanning, Guangxi, 530004, People's Republic of China

† Electronic supplementary information (ESI) available: Experimental details including synthesis, the characterization of the compounds, absorption and fluorescence spectroscopic data, and living cells imaging. See DOI: 10.1039/d0nj05900e

changes in the polarity of LDs in cancer development projects. However, the predominated challenge in constructing such optical agents is to control their luminescent behavior at different polarities in systems. Ideally, the tumors should be obviously discriminated from normal cells according to the difference in their fluorescence signals caused by LDs' polarity variance. Another concern is to ensure that the probe is primarily located in LDs to avoid false signals from other suborganelles because the local polarity differs considerably from one region to another. With polarity-sensitive and LDs targeting optical agents, the contribution of LDs' polarity in tumor development could be revealed. However, to the best of our knowledge, such a powerful probe has not been proposed for exploring the potential role of LDs polarity in the cancer evolution.

In this work, we designed and synthesized a new fluorescent probe CTPE with 3-acetyl-7-(*N,N*-diethyl)amino benzopyran-2-one (the coumarin dye) as the polarity sensitive dye, with tetraphenylethylene (TPE) as the electron donor. The probe has excellent LDs targeting ability, good photo-stability and a low biological toxicity. Owing to the intramolecular charge transfer (ICT), CTPE exhibited a good solvation effect. As anticipated, the probe displayed a stronger fluorescence in cancerous tissues and a weaker fluorescence in the normal tissues. Thus, cancer and normal tissues can be clearly discriminated by fluorescence signals. Using this probe, the LDs polarity in the evolution of cancer has been successfully explored. In addition, LDs polarity fluctuations in cells incubated with different stimulants have been detected.

## 2. Experimental

### 2.1. Materials and instruments

Unless otherwise stated, ultrapure water was utilized in the experiments. Solvents were of spectral purity. All instruments utilized in the research are illustrated in the ESI.†

### 2.2. Synthesis of CTPE

The synthetic route and part of the synthesis processes are displayed in the ESI.† Compound 1 and compound 2 were dissolved in 10 mL of solvent (ethanol) and three drops of piperidine were added as a catalyst. Then, the mixture was protected by nitrogen and refluxed at 80 °C for 24 h. After the reaction was complete, the solution was cooled to room temperature and the solvent in the reaction system was distilled off under reduced pressure. The crude product was purified by column chromatography (methanol : dichloromethane = 1 : 50), and finally a red solid was obtained. <sup>1</sup>H NMR (400 MHz, chloroform-*d*) δ 8.53 (s, 1H), 8.01 (d, *J* = 15.7 Hz, 1H), 7.74 (d, *J* = 15.6 Hz, 1H), 7.44 (dd, *J* = 22.5, 8.3 Hz, 3H), 7.13–7.01 (m, 15H), 6.79 (d, *J* = 8.3 Hz, 1H), 6.63 (s, 1H), 5.30 (s, 1H), 3.47 (q, *J* = 7.1 Hz, 4H), 1.26 (t, *J* = 7.0 Hz, 7H). <sup>13</sup>C NMR (101 MHz, chloroform-*d*) δ 186.43, 160.86, 158.68, 152.95, 148.63, 146.12, 143.54, 143.44, 143.36, 143.10, 141.89, 140.37, 133.46, 128.20, 127.86, 127.77, 127.66, 126.80, 126.62, 126.57, 124.52, 116.86,

109.89, 108.69, 96.69, 45.20, 12.50. HR-MS *m/z*: calcd for C<sub>42</sub>H<sub>35</sub>NO<sub>3</sub> 602.27; found, 602.2693.

### 2.3. General procedures for spectral test

The 1 mM CTPE stock solution was prepared in dimethyl sulfoxide (DMSO). Toluene, dioxane, dichloromethane (DCM), acetone, *N,N*-dimethylformamide (DMF) used in the experiment were all spectrally pure. Before performing the spectrum test, the solutions used were thoroughly shaken. All measurements were performed using 420 nm excitation and 5.0 nm excitation/emission gap width parameters.

### 2.4. Cell culture and imaging methods

The 4T1, HepG2, and HeLa cancer cells were used in this work. Dulbecco's Modified Eagle Medium media (DMEM, Hyclone) supplemented with 10% heat-inactivated fetal bovine serum (FBS, Sijiqing) and 1% antibiotics (100 U mL<sup>-1</sup> penicillin and 100 μg mL<sup>-1</sup> streptomycin, Hyclone) were utilized for cells culture at 37 °C and 5% CO<sub>2</sub>. Before imaging, 1 mL cells were seeded in glass bottom culture dishes (Nest) at a density of 1 × 10<sup>5</sup> mL<sup>-1</sup>. These cells were loaded on glass coverslips and allowed to adhere for 24 h. After the cells were covered about 70% confluence, imaging experiments were carried out. For imaging cells, 10 μL CTPE were mixed with 1 mL culture medium firstly and then utilized for incubating cells for 30 min. Before imaging, cells were washed 3 times with PBS to remove the residual probe. Finally, confocal fluorescence imaging was carried out by Nikon fluorescence microscope equipped with 100× objective lens.

### 2.5. Fluorescent imaging in tumor tissues and normal organs tissues

Five-week-old female balb/c mice were purchased from the School of Pharmaceutical Sciences, Shandong University, and the studies were approved by the Animal Ethical Experiment Committee of Shandong University. The entire experiment followed the animal protection guidelines of the National Laboratory Animal Use Law (China). 4T1 cells were transplanted into mice to establish tumor models. These normal mouse organs (heart, liver, spleen, lung, kidney) and tumor of tumor-bearing mice were isolated, respectively, and wash them with PBS (pH 7.4) thrice. With the help of a vibrating blade microtome, the slices were cut to 200 μm thickness in 25 mM PBS (pH 7.4). Then, these slices were incubated with 15 μM CTPE in PBS buffer for 2 h with 95% O<sub>2</sub> and 5% CO<sub>2</sub> at 37 °C. After washing three times with PBS, these samples were transferred to a glass bottom dish and observed under a confocal microscope.

## 3. Results and discussion

### 3.1. Design strategy of the probe CTPE

The donor (D)-π-acceptor (A) structure is generally beneficial for polarity sensitivity and the hydrophobic nature is favorable for LDs targeting.<sup>28</sup> Based on this, 3-acetyl-7-(*N,N*-diethyl) amino benzopyran-2-one (the coumarin dye) was selected as a

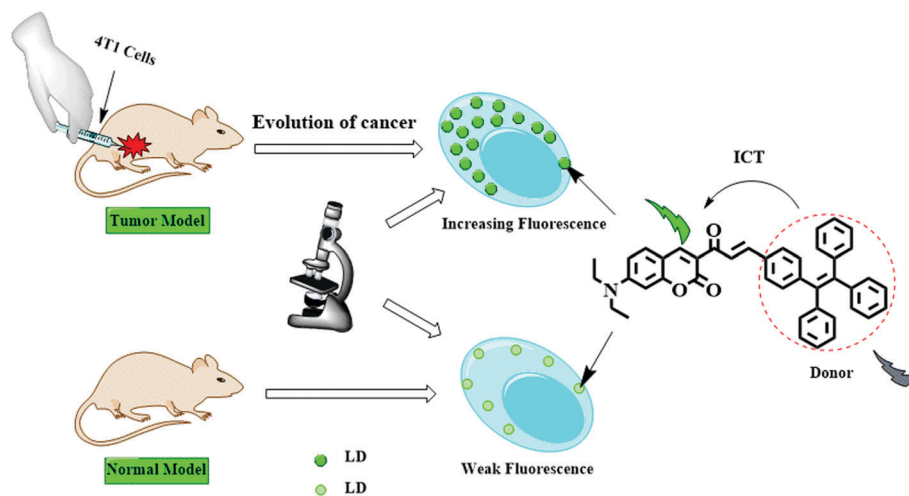


Fig. 1 The design concept of the probe CTPE for monitoring LDs polarity in cancer cells and normal cells.

fluorophore because it shows substantial changes in the dipole moments while undergoing electronic transitions, and therefore can serve as polarity-sensitive dye.<sup>29</sup> Tetraphenylethylene (TPE) plays the role of electron donor in CTPE probe, and the introduction of TPE increases the conjugation in CTPE as evidenced by red shift, which makes it more suitable for biological imaging.<sup>30</sup> According to our assumption, the fluorescence intensity of the probe with this push-pull electronic structure will be sensitive to polarity.<sup>31,32</sup> We anticipated that owing to the LDs polarity variance caused by specific alterations in metabolism of cancer, the probe will exhibit stronger fluorescence in cancer tissues and weaker in normal tissues. Moreover, with the development of the tumor, the LDs polarity of the tumor tissue

may change, and this change will be manifested by the fluorescence intensity of the tissue incubated with CTPE (Fig. 1).

### 3.2. Optical properties of CTPE

The absorption and fluorescence spectra of CTPE in solvents such as toluene, dioxane, dichloromethane (DCM), acetone, and *N,N*-dimethylformamide (DMF) were analyzed. As shown in Fig. 2a, the absorption wavelength of CTPE in solvents of different polarities were slightly red shifted from 456 nm of toluene to 464 nm of DMF. In the fluorescence spectra, this trend is even more obvious. As shown in Fig. 2b, the emission wavelength of CTPE ranges from 502 nm in low-polarity solvent (toluene) to 561 nm in the highly polar solvent (DMF) with a red

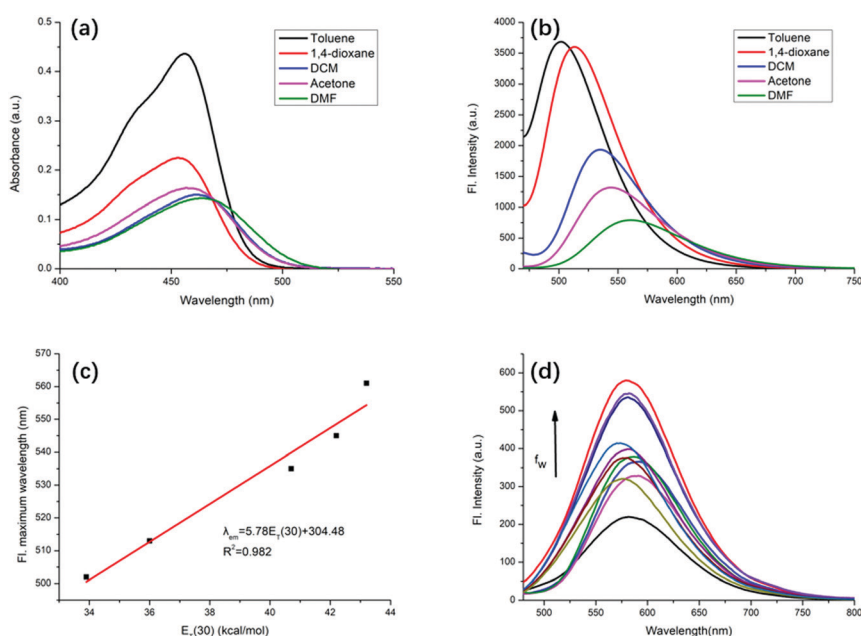


Fig. 2 (a) The absorption spectra of CTPE in solvents with various polarities. (b) The fluorescence spectra of CTPE in solvents with various polarities. (c) The plot of the emission maximum of the probe CTPE in diverse solvents versus  $E_T(30)$ . (d) Fluorescence spectra of CTPE in different ratios of methanol and glycerol system. Concentration: 10  $\mu$ M;  $\lambda_{ex}$  = 460 nm.

shift of 59 nm. Simultaneously, as shown in Fig. 2b, as the polarity of the solvent increases, the fluorescence intensity of CTPE decreases accordingly, which may be ascribed to the “positive solvatokinetic effect”.<sup>33</sup> This effect can be manifested by changes in the fluorescence quantum yield of CTPE in different solvents (Table S1, ESI<sup>†</sup>). Moreover, the fluorescent lifetime variation of the CTPE under different polarities was studied. From Fig. S1 (ESI<sup>†</sup>), it can be seen that as the solvent polarity increases, the fluorescent lifetime of the probe in different solvents gets shortened. To further understand the influence of solvent polarity on CTPE emission, a linear regression curve of the maximum emission wavelength of the probe with respect to the solvent polarity parameter  $E_T(30)$  was plotted. As displayed in Fig. 2c, an excellent linearity ( $R^2 = 0.982$ ) was obtained when the emission maximum of CTPE was plotted against the  $E_T(30)$ . This data indicated that the probe is highly dependent on polarity, which is consistent with our original probe design philosophy.

Due to the existence of single bonds in the CTPE structure, limiting the rotation of single bonds by increasing the solvent viscosity is expected to affect the fluorescence of the probe to a certain extent. To understand the influence of viscosity on the fluorescence intensity, the fluorescence spectra of CTPE in the methanol–glycerol system with different ratios were measured. As shown in Fig. 2d, with the increase of solvent viscosity, the maximum fluorescence intensity of CTPE only increased from 219.8 to 579.8, while the maximum fluorescence intensity of each solvent in Fig. 2b is mostly higher than this change. To further prove that CTPE is more sensitive to polarity, we compared the fluorescence spectra of CTPE in THF and MeOH solvent mixture (Fig. S2, ESI<sup>†</sup>), which have similar viscosities but different polarities. The fluorescence spectrum of CTPE in this system significantly changed. The above results show that the sensitivity of CTPE probe to polarity is much higher than that of viscosity of the solution. In other words, the change in the probe fluorescence intensity with viscosity is basically negligible. Therefore, we believe that CTPE could be utilized to detect the polarity change despite being in viscous media.

Living biological cells are a very complex system that contains a variety of biological macromolecules and a variety of ions. To detect the selectivity of probe polarity in such a complex environment, the fluorescence spectra of the probe CTPE in the presence of Gln, Thr, Cys, Gly, Asn and other biological macromolecules, and various ions were collected. As shown in Fig. S3 (ESI<sup>†</sup>), the fluorescence of the probe did not change significantly indicating that the probe was not influenced by these biomolecules and ions. In addition, the result of probe in different pH solutions demonstrated that CTPE is essentially pH-insensitive over the pH range of 3.0–10.0 (Fig. S4, ESI<sup>†</sup>). These results indicate that CTPE has high selectivity and can detect changes in polarity in more complex environments. In the photo stability experiment (Fig. S5, ESI<sup>†</sup>), it can be seen that the fluorescence intensity of CTPE hardly changes with time even under continuous irradiation of 90 min, which proves its excellent photo-stability. Furthermore, to verify the biological toxicity of CTPE, the MTT assay was introduced to establish the

cytotoxicity test of the probe in HepG2, HeLa and 4T1 cells (Fig. S6, ESI<sup>†</sup>). The results show that even when the probe concentration is 50  $\mu\text{M}$ , the survival rate could still reach over 80%. The above results show that the probe CTPE has high selectivity, low biological toxicity and a good photo-stability, therefore making it an excellent tool for detecting polarity in complex biological systems.

### 3.3. Co-localization experiments

Subsequently, the commercial dye Nile red and CTPE were used for colocalization experiments. An ideal condition was explored first to ensure that green fluorescence only came from the probe CTPE (Fig. 3a), and red fluorescence (Fig. 3b) only came from Nile red. HepG2, HeLa, 4T1 cells were co-cultured with CTPE and Nile red at the same time. As shown in Fig. 3c, we observed granular dots in both red and green channels, which is a typical shape for LDs (Fig. 3c). Moreover, yellow fluorescence was observed in the merge image, indicating that the two channels have a large overlap, and the correlation of the intensity scatter plot reached 0.92. All these results indicate that the probe has the property of locating LDs in cells, and CTPE is capable of monitoring the changes in polarity of LDs in living cells.

### 3.4. Imaging LDs polarity under abnormal physiological state

The polarity of LDs in cells under abnormal physiological conditions was further monitored by confocal microscopy. As shown in Fig. 4a, the cells were incubated with CTPE for 1 hour. Granular LDs were seen in the cells and appropriate fluorescence intensity was observed. Previous reports have shown that when fatty acids (such as oleic acid) are added to the cell culture medium, the number and size of LDs changes due to the stimulation of the fatty acid receptor FFAR4.<sup>34,35</sup> Herein, 10  $\mu\text{L}$

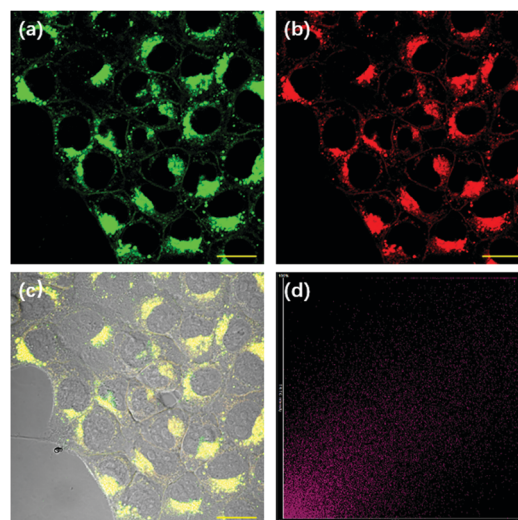


Fig. 3 The co-localization fluorescence images of CTPE in 4T1 cells. (a) CTPE (1  $\mu\text{M}$ ) stain. (b) Nile red (2.0  $\mu\text{M}$ ) stain. (c) Merged image of (a) and (b). (d) The intensity scatter plot of two channels. Scale bar: 20  $\mu\text{m}$ . Green channel:  $\lambda_{\text{ex}} = 488$  nm, collected 500–550 nm. Red channel:  $\lambda_{\text{ex}} = 561$  nm, collected 570–620 nm.

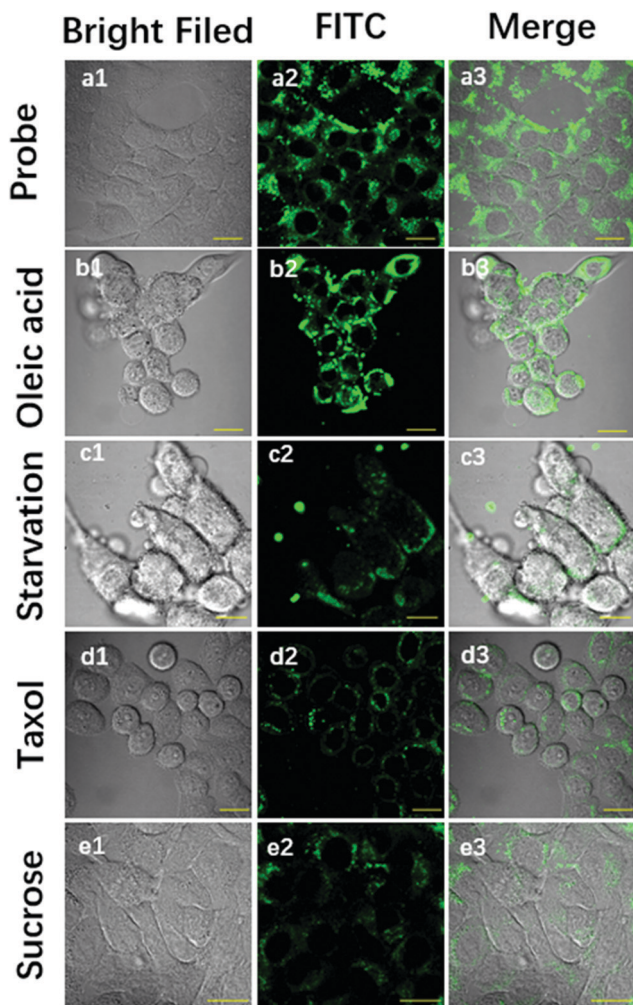


Fig. 4 Fluorescence imaging of 4T1 cells. (a1–a3) 4T1 cells incubated with 10  $\mu\text{M}$  probe CTPE for 30 min; (b1–b3) 4T1 cells incubated with 20  $\mu\text{M}$  oleic acid for 1 h and 10  $\mu\text{M}$  CTPE for another 30 min (c1–c3) 4T1 cells were incubated with PBS for 24 hours and 10  $\mu\text{M}$  CTPE for another 30 min; (d1–d3) 4T1 cells incubated with 20  $\mu\text{M}$  taxol for 30 min and 10  $\mu\text{M}$  CTPE for another 30 min. (e1–e3) 4T1 cells incubated with 20  $\mu\text{M}$  sucrose solution for 30 min and 10  $\mu\text{M}$  CTPE for another 30 min. Conditions:  $\lambda_{\text{em}} = 500\text{--}550\text{ nm}$ ;  $\lambda_{\text{ex}} = 488\text{ nm}$ . Scale bar: 20  $\mu\text{m}$ .

of oleic acid was added to the medium and then incubated with probe for 1 hour and imaged. Simultaneously, the cells that were only incubated with the probe were set as control group. Compared with the control group (a1–a3), the number and volume of LDs increased, hence, the fluorescence intensity of LDs increased after incubation with oleic acid (Fig. 4b). The results show that besides polarity CTPE can also dynamically monitor the number and size of LDs in living cells.

In addition, detecting the polarity changes in LDs of cells in different states is necessary to understand the pathological process of LDs-related diseases. Therefore, three models of abnormal cell state were established to detect changes in LDs' polarity. In detail, PBS (pH = 7.4) was utilized to culture 4T1 cells instead of another medium to produce starvation. As shown in Fig. 4c, in the state of starvation, the probe exhibited weaker fluorescence compared with control group (Fig. 4a).

Similarly, weak fluorescence was also observed in taxol (Fig. 4d) and sucrose (Fig. 4e) treated group. The results demonstrated that the LDs' polarity will decrease in abnormal cell state. Moreover, similar phenomena were obtained in HeLa and HepG2 cells (Fig. S7 and S8, ESI<sup>†</sup>). Thus, we believe that CTPE can dynamically monitor the LDs' polarity in cells under different conditions.

### 3.5. Fluorescence imaging of LDs polarity in the evolution of cancer

Based on the above detection results for abnormal cells, we tried to further explore the changes in the polarity of LDs during the evolution of cancer in the tissues. Four different mouse tumor models were established (Fig. S9, ESI<sup>†</sup>). 4T1 cells were inoculated into normal mice to establish a tumor model, and the tumor tissues were obtained after 2 days, 5 days and 10 days, respectively. Concurrently, 20  $\mu\text{L}$  taxol was injected to 8 day-tumor mice as a treatment group and the proposed slices were obtained after 2 days of treatment (Fig. 5). The above tissues were sliced in PBS. After CTPE staining, granular bright spots could be seen in the tumor tissue, which is a typical shape of LDs, indicating that CTPE could still locate LDs in the tissue.

As expected, the polarity of LDs in tumor tissue changed with the time of inoculation, and this change is reflected by the fluorescence brightness after CTPE staining. This indicates that as the tumor develops, the number of LDs gradually decreased. Note that, after drug treatment, the fluorescence intensity of tumor decreased significantly compared with the 10 day-tumor slices, indicating that the LDs polarity increased. The above results revealed that with the evolution of cancer, the polarity of LDs in tumor tissue gradually decreases, and after the treatment, the polarity in tumor tissue increases again.

In addition, the penetration ability of the probe in different organ tissues (heart, liver, spleen, lung, kidney) was examined, and the fluorescence could still be observed at a depth of 50  $\mu\text{m}$

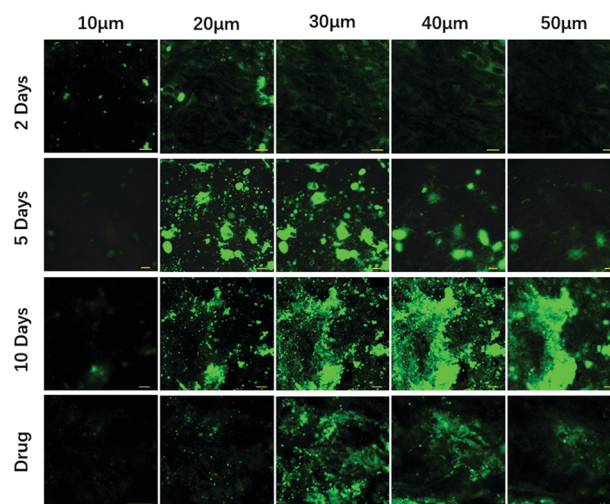


Fig. 5 The imaging of mouse tumors slices of different periods and drug-treated tumors slices with CTPE (10  $\mu\text{M}$ ) at a depth of 10–50  $\mu\text{m}$ . The fluorescence was collected at 500–550 nm with 488 nm excitation.

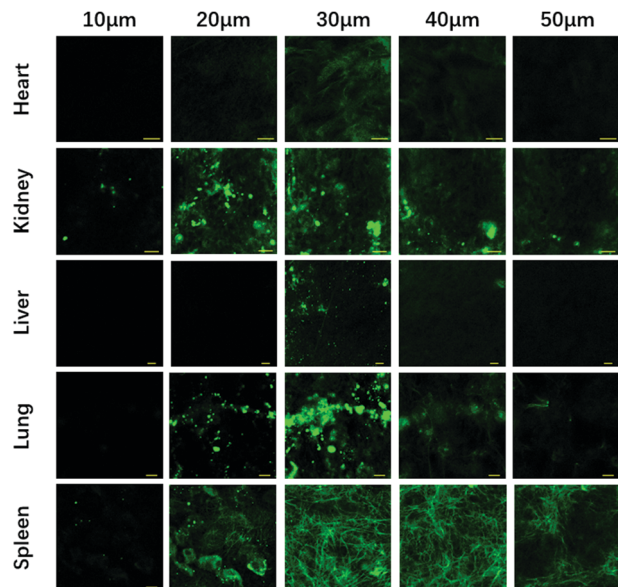


Fig. 6 The imaging the subcutaneous tissue sections of inflammatory mice and normal mice pretreated with CTPE (10  $\mu$ M) with a depth of 10–50  $\mu$ m. Fluorescence was collected at 500–550 nm under excitation at 488 nm.

confirming a good penetration depth of CTPE (Fig. 6). In a nutshell, this work demonstrated that the probe can be used as a powerful tool for cancer diagnosis and for tracking therapeutic efficacy by detecting LDs polarity.

### 3.6. Fluorescence imaging of LDs polarity in the inflammation mice

In addition, the inflammatory mouse model was established to explore the change of the polarity of LDs. Through intraperitoneal injection of 20  $\mu$ L lipopolysaccharide (LPS), a mouse model of acute inflammation was obtained after 24 h, and a subcutaneous tissue section of the abdominal cavity was taken. After adding CTPE staining for 2 h, imaging was performed using a confocal microscope, and granular LDs could be seen in the imaging results (Fig. 7). By comparing with the subcutaneous tissue of normal mice, it could be seen that the fluorescence in the inflamed tissue was stronger than that in the normal tissue and the number of LDs in the inflammation model was higher

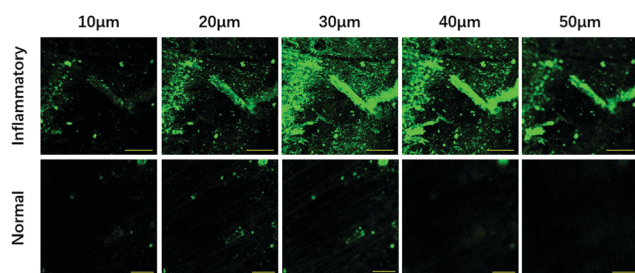


Fig. 7 The imaging the subcutaneous tissue sections of inflammatory mice and normal mice pretreated with CTPE (10  $\mu$ M) with a depth of 10–50  $\mu$ m. Fluorescence was collected at 500–550 nm under excitation at 488 nm.

than the other. This indicates that the polarity of LDs in inflamed tissues is lower than that in normal tissues; with the occurrence of inflammation, the number of LDs also increased.

Finally, to ensure that the fluorescence in tissue imaging is entirely from CTPE, we used confocal microscopy to image the tissue without CTPE staining under the same parameters, and only negligible fluorescence was found in the imaging results (Fig. S10, ESI<sup>†</sup>).

## 4. Conclusion

In summary, we designed and synthesized a new polar fluorescent probe CTPE targeting LDs and explored the LD polarity of cancer tissues at different stages. In addition to their targeting ability, CTPE also exhibited a good biocompatibility and photo stability. Due to the donor- $\pi$ -acceptor structure of CTPE, the probe displayed a high sensitivity towards the polarity of the environment, endowing CTPE the ability to specifically detect the polarity of LDs in living cells. By means of the probe, the LDs' polarity in cells as induced by PBS, sucrose and taxol was successfully sensed. More importantly, in virtue of the CTPE, the change trend of the polarity of LDs during the evolution of cancer was explored, and the therapeutic effects of paclitaxel were also tracked. We believe that CTPE has the potential to become a powerful tool for exploring pathological changes in the development of cancer.

## Conflicts of interest

There are no conflicts to declare.

## Acknowledgements

This work was financially supported by NSFC (21672083, 21877048, 22077048), Taishan Scholar Foundation (TS201511041), and the startup fund of the University of Jinan (309-10004).

## Notes and references

- 1 R. L. Siegel, K. D. Miller and A. Jemal, *Ca-Cancer J. Clin.*, 2016, **66**, 7.
- 2 T. E. Byers, H. J. Wolf and K. R. Bauer, *et al.*, *Cancer*, 2010, **113**(3), 582–591.
- 3 R. D. Neal, P. Tharmanathan and B. France, *et al.*, *Br. J. Cancer*, 2015, **112**, S92–S107.
- 4 P. C. Boutros, *Genome Res.*, 2015, **25**(10), 1508–1513.
- 5 M. Chiba, Y. Ichikawa, M. Kamiya, T. Komatsu, T. Ueno, K. Hanaoka, T. Nagano, N. Lange and Y. Urano, *Angew. Chem., Int. Ed.*, 2017, **56**, 10418–10422.
- 6 M. Gao, F. Yu, C. Lv, J. Choo and L. Chen, *Chem. Soc. Rev.*, 2017, **46**, 2237–2271.
- 7 B. Daniele, A. Bencivenga, A. S. Megna and V. Tinessa, *Gastroenterology*, 2004, **127**, S108.
- 8 R. V. Farese and T. C. Walther, *Cell*, 2009, **139**, 855–860.

- 9 S. Martin and R. G. Parton, *Nat. Rev. Mol. Cell Biol.*, 2006, **7**, 373–378.
- 10 T. C. Walther and R. V. Farese, Jr., *Annu. Rev. Biochem.*, 2012, **81**, 687–714.
- 11 H. S. Finstad, C. A. Drevon and M. A. Kulseth, *et al.*, *Biochem. J.*, 1998, **336**(2), 451–459.
- 12 S. O. Olofsson, P. Bostrom, L. Andersson, M. Rutberg, J. Perman and J. Boren, *Biochim. Biophys. Acta*, 2009, **1791**, 448–458.
- 13 T. C. Walther and R. V. Farese, *Annu. Rev. Biochem.*, 2012, **81**, 2821–2828.
- 14 S. Martin and R. G. Parton, *Nat. Rev. Mol. Cell Biol.*, 2006, **7**, 373–378.
- 15 M. Nagayama, T. Uchida and K. Gohara, *J. Lipid Res.*, 2007, **48**, 9–18.
- 16 R. Bartz, W. H. Li, B. Venables, J. K. Zehmer, M. R. Roth, R. Welti, R. G. W. Anderson, P. S. Liu and K. D. Chapman, *J. Lipid Res.*, 2007, **48**, 837–847.
- 17 C. Thiele and J. R. Spandl, *Curr. Opin. Cell Biol.*, 2008, **20**, 378–385.
- 18 O. J. Warburg, *Cancer Res.*, 2009, **9**, 148–163.
- 19 O. Warburg, *et al.*, *Biochemica*, 1924, **152**, 319–344.
- 20 Z. Zhang, Z. Yao, Y. Chen, L. Qian, S. Jiang, J. Zhou, J. Shao, A. Chen, F. Zhang and S. Zheng, *Biomed. Pharmacother.*, 2018, **97**, 339–348.
- 21 F. Baenke, B. Peck, H. Miess and A. Schulze, *Dis. Model Mech.*, 2013, **6**, 1353–1363.
- 22 C. Ghosh, S. Nandi and K. Bhattacharyya, *Chem. Phys. Lett.*, 2017, **670**, 27–31.
- 23 R. Chowdhury, M. A. Amin and K. Bhattacharyya, *J. Phys. Chem. B*, 2015, **119**, 10868–10875.
- 24 H. Abramczyk, J. Surmacki, M. Kopec, A. K. Olejnik, K. Lubecka-Pietruszewska and K. Fabianowska-Majewska, *Analyst*, 2015, **140**, 2224–2235.
- 25 J. R. Lakowicz, *Die Naturwissenschaften*, 1991, **78**(10), 456.
- 26 A. T. Aron, K. M. Ramos-Torres, J. A. Cotruvo Jr and C. J. Chang, *Acc. Chem. Res.*, 2015, **48**, 2434.
- 27 B. Dong, X. Song, X. Kong, C. Wang, Y. Tang, Y. Liu and W. Lin, *Adv. Mater.*, 2016, **28**, 8755.
- 28 S. L. Chen, L. N. Yang and Z. S. Li, *J. Chem. Phys.*, 2013, **223**, 86.
- 29 B. R. Masters, *J. Biomed. Opt.*, 2013, **18**(3), 9901.
- 30 Z. Yang, J. Cao, Y. He, J. H. Yang, T. Kim, X. Peng and J. S. Kim, *Chem. Soc. Rev.*, 2014, **43**, 4563.
- 31 S. Sasaki, Y. Niko and A. S. Klymchenko, *et al.*, *Tetrahedron*, 2014, **70**(41), 7551–7559.
- 32 T. Fujimoto and R. G. Parton, *Perspect. Biol.*, 2011, **3**, 4838–4855.
- 33 M. J. Jiang, X. G. Gu and B. Z. Tang, *et al.*, *Chem. Sci.*, 2013, **8**, 5400–5446.
- 34 O. D. Young and W. Evelyn, *Front. Endocrinol.*, 2014, **5**, 115.
- 35 A. Rohwedder, Q. Zhang, S. A. Rudge and M. J. Wakelam, *Cell Sci.*, 2014, **127**, 3104.